Cascade Exotherms for Rapidly Producing Hybrid Non-Isocyanate Polyurethane Foams from Room Temperature Formulations

Maxime Bourguignon,[a] Bruno Grignard,[ab] Christophe Detrembleur[ac*]

[a]Center for Education and Research on Macromolecules (CERM), CESAM Research Unit, University of Liege, Sart-Tilman B6a, 4000 Liege, Belgium

[b]FRITCO$_2$T Platform, University of Liege, Sart-Tilman B6a, 4000 Liege, Belgium

[c]WEL Research Institute, avenue Pasteur, 6, 1300 Wavre, Belgique

* Corresponding authors: **E-mail:** Christophe.detrembleur@uliege.be

Abstract

For decades, self-blown polyurethane foams - found in an impressive range of materials - are produced by the toxic isocyanate chemistry and are difficult to recycle. Producing them in existing production plants by a rapid isocyanate-free self-blowing process from room temperature (RT) formulations is a long-lasting challenge. The recent water-induced self-blowing of non-isocyanate polyurethane (NIPU) formulations composed of a CO_2-based tri-cyclic carbonate, diamine, water and a catalyst, successfully addressed the isocyanate issue, however failed to provide foams at RT. Herein, we elaborate a practical solution to empower the NIPU foam formation in record timeframes from RT formulations. We generate cascade exotherms by the addition of a highly reactive triamine and an epoxide to the formulation of the water-induced self-foaming process. These exotherms, combined to a fast crosslinking imparted by the triamine and epoxide, rapidly raise the temperature to the foaming threshold and deliver hybrid NIPU foams in 5 minutes with KOH as catalyst. Careful selection of the monomers enables producing foams with a wide range of properties, as well as with an unprecedented high bio-based content up to 90 wt%. Moreover, foams can be upcycled into polymer films by hot-pressing, offering them a facile reuse scenario. This robust cheap process opens huge perspectives for greener foams of high bio-based contents, expectedly responding to the sustainability demands of the foam sector. It is potentially compatible to the retrofitting of industrial foaming infrastructures, which is of paramount importance to accommodate existing foam production plants and address the huge foam market demands.

Introduction

With a global market estimated to 49.5 billion USD in 2023,[1] polyurethane foams are essential materials of our modern life with multiple usages in thermal and sound insulation, as items for comfort and furniture (seats and mattresses), etc. [2,3] Pushed by an estimated market growth of 7.4% for the 2022-2027 period,[4] the success of PU foams stems from their ease of fabrication from low-cost isocyanates and polyols. Beside the formation of urethane linkages by addition of the polyisocyanate with the polyol, the addition of water within the reactive formulation causes the partial hydrolysis of the isocyanate leading to the *in-situ* delivery of CO_2 acting as the blowing agent.[5] However, due to their acute toxicity,[6,7] isocyanates face REACH restrictions of use.[8] Besides, the new EU policies on the decarbonization of the plastic sector encourage the exploitation of raw chemicals issued from bio-origin and/or gaseous waste effluents such as CO_2.[9] As a result, these incentives provide a new impetus to engineer ways of producing isocyanate-free polyurethane foams while meeting the sustainability objectives of our modern society.

In the last decade, the polyaddition of polyamines with poly(cyclic carbonate)s into poly(hydroxyurethane)s (PHU) has emerged as one of the main greener alternatives to conventional PUs.[10–12] PHUs foaming was previously achieved by using blowing agents such as a fluorinated solvent (Solkane),[13] supercritical CO_2,[14] or inorganic carbonate salts like K_2CO_3 and $NaHCO_3$ that release CO_2 when combined with maleic or acetic acid.[15l,16] The first self-blown PHU foams was described with Momentive MH15, a poly(methylhydrogensiloxane), that released *in-situ* highly flammable H_2 as the blowing agent when reacting with the polyamine.[17–20] However this foaming strategy faces safety issues. In a recent and safer approach, Choong illustrated the formation of self-blown PHU by utilizing some amine/CO_2 adducts at moderate temperature (50-60 °C), however the process required long reaction times (24-48 h).[21] To date, most of these foaming approaches are difficult to implement at the industrial scale, and are not mimicking the PU self-blowing technology where the isocyanate serves both to construct the polymer matrix and to generate the blowing agent (i.e. CO_2). In 2018, North pioneered the concept of CO_2 self-blown PHU foams by designing a specific sorbitol-derived biscyclic carbonate responding to this dual function.[22] However, the CO_2 was produced by an intramolecular decarboxylative rearrangement specific to this monomer rending the process non-versatile. In 2020, our group pushed forward the CO_2 self-blown PHU technology by promoting divergent ring-opening reactions of the cyclic carbonate.[23] The nucleophilic attack of the carbonyl site by the amines formed the hydroxyurethane linkages while a competitive S-alkylation reaction delivered CO_2 *via* attack of the methylene site by thiols added to the formulation. The foaming however occurred at 100-120 °C for hours. The process temperature was decreased to 80-90 °C by utilizing masked thiols that released in-situ the thiols needed for the S-alkylation (Scheme 1A).[24,25] Process optimizations by decoupling the crosslinking of the network and the material expansion provided expanded materials in 30 min, however at 120 °C.[26]

In 2022, we demonstrated that a tiny amount of water introduced in a PHU formulation was able to generate the foaming *via* hydrolysis of the cyclic carbonate that generated CO_2 (Scheme 1A).[27] Although very broad in scope, this technology requested 30 min to deliver the foams when the formulation components were pre-heated at 100 °C. It was

thus well suited to produce foams by the reactive injection molding (RIM) technology where molds are most often heated. However, it was still not competitive with PU foam manufacturing requiring short reaction times (2 to 10 min) at room temperature (e.g. for producing mattresses or sandwiched panels). Due to the low reactivity of the cyclic carbonates compared to isocyanates, the objective of fast foaming of PHUs from room temperature formulations appeared very challenging. Herein, we demonstrate that the water-induced self-foaming PHU technology can compete the conventional PU one, with a fast foaming (i.e. 5 min) from room temperature (RT) formulations (Scheme 1B). To reach this goal, we addressed two main questions: 1) *how to bypass the low cyclic carbonate reactivity to reach short foaming times*, and 2) *how to initiate this fast foaming from RT formulations*. The first issue was tackled by merging rheology analyses, infrared spectroscopy characterizations and gel content measurements of the foams. These experiments allowed the identification of the main bottlenecks of the PHU foaming process, yet proposing the main experimental actions to accelerate the foaming process, from 30 to 5 minutes starting from formulations pre-heated at 100 °C. Then, the challenging fast foaming from RT formulations was overcome by combining a highly reactive primary amine crosslinker, affording a fast crosslinking, to cascade exothermic reactions that rapidly increased the formulation temperature to the foaming zone. This simple technology provides foams with tunable rigidity and is compatible with a wide range of bio-based comonomers, enabling to produce foams with a theoretical bio-renewable content up to 90 wt%. Moreover, the PHU thermoset foams were easily upcycled into second-life materials (e.g. polymer films) by hot pressing. This foaming technology is thus of high potential to produce the next generation of more sustainable recyclable PU foams while accommodating the existing PU foaming infrastructures, paving the way for greener foams meeting the huge demands of the market.

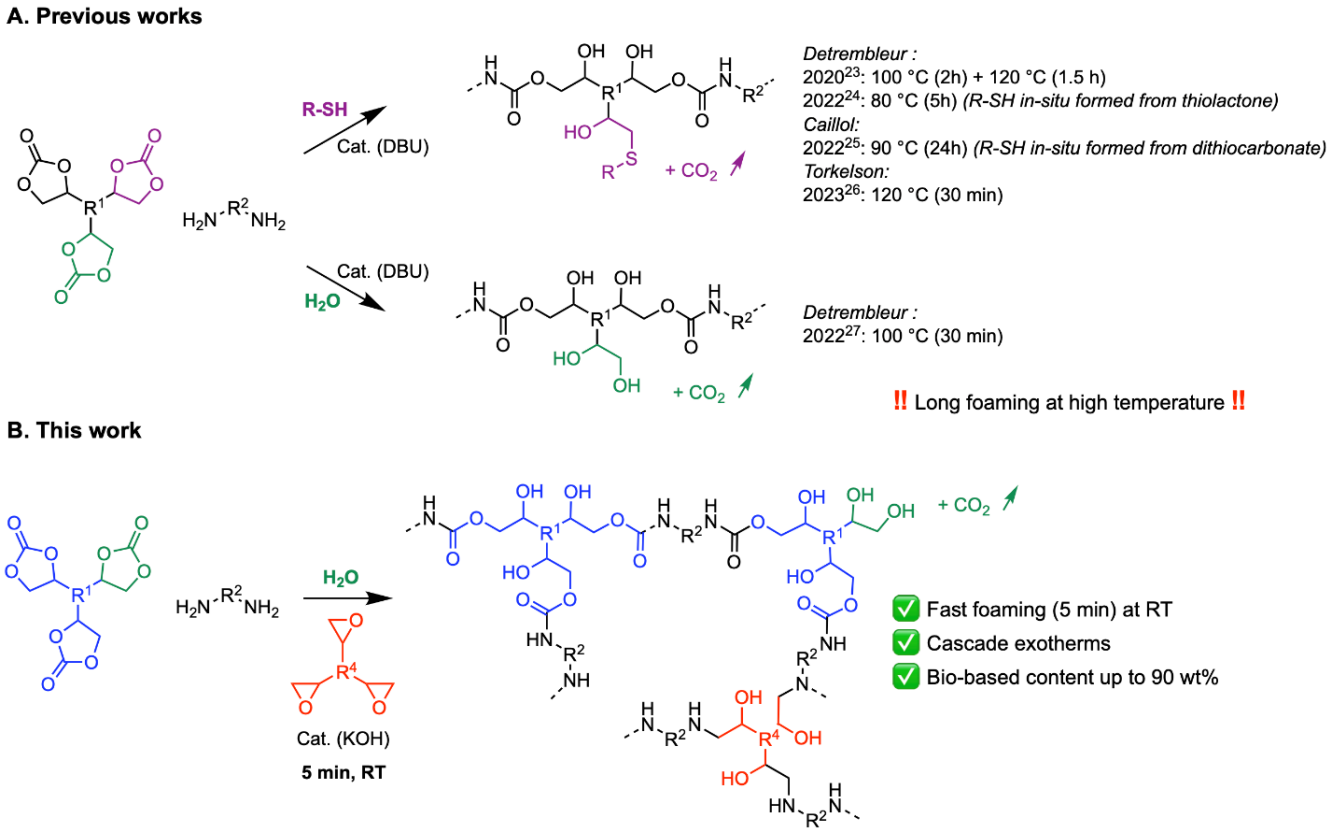

Scheme 1. Comparison of the strategies to produce self-blown non-isocyanate polyurethane foams by utilizing the cyclic carbonate as the comonomer and the precursor of the blowing agent (CO_2): (A) the thiol- and water-induced based processes, and (B) the hybrid one. Simplified structures for clarity.

Experimental section

Products

Trimethylol propane triglycidyl ether (TMPTE, Aldrich, technical grade), Butanediol diglycidyl ether (BDGE, Aldrich > 95%) DER 332™ (Aldrich), Neopentyl glycol diglycidyl ether (ABCR, technical grade), Glycerol triglycidylether was kindly provided by Ipox (IPOX CL 12), m-xylylene diamine (XDA, Aldrich, 99%), 1,2-Bis(2-aminoethoxy)ethane (EDR 148, TCI, >98%), Hexamethylene diamine (HMDA, Aldrich, 98%), 1,3-Bis(aminomethyl)cyclohexane (cis-and trans -mixture) (1,3 BAC, TCI, 98%), Benzylamine (Aldrich, 99%), potassium hydroxide (KOH, VWR, 90%), Tris(2-aminoethylamine) (TREN, Aldrich, 96%). Tetrabutylammonium iodide (TBAI, Aldrich, 99%), Hydrotalcite synthetic ($Mg_6Al_2(CO_3)(OH)_{16}{\cdot}4H_2O$, Aldrich), Cloisite Na (Sauthern clay). The different cyclic carbonates were produced from CO_2 fixation onto the corresponding epoxides. Their syntheses at the kg-scale and characterizations are shown in Figures S47 to S49

Methods and characterizations.

Rheological experiments were carried out in isothermal mode with a frequency of 1 Hz and initial strain of 1%, and under the auto tension adjustment mode (axial force of 10 g) that allowed gap to increase (Delta L) when the foam expanded. The Delta L was continuously measured and reported in % of the max delta L and depicted as Expansion (%) in Figure S1. The start of the foaming was defined as the time to reach 5% of the maximum expansion. Gel point was defined by the crossover between G' and G''. The rheometer and the 25 mm parallel plates were preheated at 100 °C. The components of the formulation were preheated at 100 °C separately, then rapidly mixed manually and finally, placed to 25 mm parallel plates of the rheometer. All parameters (foam expansion, G' and G'', viscosity) were simultaneously recorded over time at 100 °C. Results are discussed in Figure 1.

Gel contents were measured in triplicate by incubating foam samples of more or less 200 mg in 20 mL of THF for 24h according to the following formula $GC = 100\, x \frac{m_2}{m_1}$, where m_1 and m_2 are mass before immersion and mass after immersion and drying until constant weight, respectively.

Overall foam density was assessed by weighting whole foam and divided it by its volume. The core density was measured by cutting three cubes (± 1.5 x 1.5 x 1.5 cm) in the center of the foam at different location in the foam (1/3, 1/2 and 2/3 of the height in the direction of the expansion). The cubes were measured and weighted. Core density was calculated at the mean of the individual density.

ATR spectra were measured by using a Nicolet IS5 spectrometer (Thermo Fisher Scientific) equipped with a transmission or with a diamond attenuated transmission reflectance (ATR) device. Spectra were obtained in transmission or ATR mode as a result of 32 spectra in the range of 4000–500 cm^{-1} with a nominal resolution of 4 cm^{-1}. Spectra were analyzed with an ONIUMTM (Thermo Fisher Scientific) software. Analyses were carried out on the inner part of the foam after removing the foam skin.

Nuclear magnetic resonance (NMR) spectroscopy.^{1}H-NMR analyses were performed on Bruker Avance 400 MHz spectrometers at 25 °C in the Fourier transform mode in deuterated solvent ($CDCl_3$ or DMSO d6)

Differential scanning calorimetry (DSC) was performed on a DSC250 TA Instruments calorimeter. The equilibrated foam (48 h under ambient condition) was placed in a non-hermetic pan and $T_{g,equ}$ was measured according to the first ramp temperature (-40 °C to 80 °C at 10 °C/min).

Thermogravimetric analysis (TGA) was performed on a TGA2 instrument from Mettler Toledo. Around 10 mg of sample were heated at 10 °C/min until 600 °C under a nitrogen atmosphere (50 mL/min). $T_{d,5\%}$ was measured as the temperature at 5% mass loss starting from the mass measured at 100 °C to exclude the mass of entrapped water.

Scanning electron microscopy (SEM) was realized with a QUANTA 600 apparatus microscope from FEI. The cells size distributions was calculated by the mean diameter measurements of at least 100 cells.

Compression measurement was carried out on a Zwick Roel device equipped with the testXpert software. Sample of 1 cm x 1 cm x 1cm was pressed at a rate of 1 mm/min. Compression modulus was calculated as the slope of the stress-strain curve for strain between 1 and 6%.

Procedures for water-induced foaming in open molds

Fast foaming procedure at 100 °C. TMPTC (5 g, 5CC = 34.5 mmol) and hydrotalcite (600 mg) were mixed together in a square silicon mold (S = 16 cm^2) until the obtention of a homogeneous white mixture. The mold containing the mixture was placed in an oven at 100 °C until the mixture reached this temperature. A KOH (240 mg, 4.3 mmol)/H_2O (155 mg, 8.6 mmol) mixture was preheated at 100 °C in a closed vial for 10 min. Finally, XDA (1750 mg, NH_2 = 25.7 mmol) was preheated at 100 °C for 10 min in a closed vial. First, the amine and then the KOH solution were added and mixed to the TMPTC mechanically for approximatively 0.5 min. The foam was then cured at 100 °C for 5 min. The experiment was reproduced by varying the amine mixture first using a mix of XDA (1220 mg NH_2 = 18.2 mmol) and TREN (380 mg, NH_2 = 7.8 mmol), then a mix of XDA (1650 mg NH_2 = 24.2 mmol) and TREN (500 mg, NH_2 = 10.3 mmol). In each case, the amines were mixed together before addition in TMPTC.

Fast foaming at 100 °C with alternative greener formulations. GTC (4.5 g, 5CC = 34.5 mmol) and Cloisite Na (540 mg) were mixed together in a square silicon mold (S = 16 cm^2) until the obtention of a homogeneous white mixture. The mold containing the mixture was placed in an oven at 100 °C until the mixture reached this temperature. A KOH (240 mg, 4.3 mmol)/H_2O (155 mg, 8.6 mmol) mixture was preheated at 100 °C in a closed vial for 10 min. 1,3-BAC or HMDA (NH_2 = 24.2 mmol) and TREN (500 mg, NH_2 = 10.3 mmol) were mixed and preheated at 100 °C for 10 min in a closed vial. First, the amine and then the KOH solution were added and mixed to the GTC mechanically for approximatively 0.5 min or until the foam started to expand. The foam was then cured at 100 °C for 5 min. Rigid foam was obtained using 1,3-BAC (1722 mg, entry 10 in Table S1). Flexible foam was obtained using HMDA (1403 mg, entry 9 in Table S1).

Typical procedure for fast foaming from room temperature formulations (1 eq of TMPTE vs TMPTC). TMPTC (17.9 g, 5CC = 123 mmol, 1 eq), TMPTE (12.47 g, epoxide = 123 mmol, 1 eq) and hydrotalcite (3 g, 6.2 wt%) were added in a cylindrical plastic vial with a diameter of 5 cm, and were then mixed together for 2 min until a homogeneous mixture was obtained. The amine mixture was then added (XDA 10.3 g, NH_2 = 151 mmol, 1.23 eq and TREN 3.17g, NH_2 = 65 mmol, 0.52 eq) to the TMPTC/TMPTE/hydrotalcite mixture and briefly mixed manually until an homogeneous mixture was obtained. Finally, an aqueous solution of KOH was prepared by solubilizing KOH (0.87 g, 15.4 mmol, 0.125 eq vs 5CC) in water (0.56 g, 1.2 wt% 31 mmol, 0.25 eq vs 5CC) and added to the foaming formulation to initiate the foaming. After mixing manually briefly, foam was let to expand at room temperature. The contents of the different components for preparing PHU foams with the different TMPTC/TMPTE ratios were presented in Table S2 and S3. The hybrid PHU/epoxide foams with different amines or epoxides presented in Figure 6 are prepared according to the same procedure with quantities reported in Table S5.

Monitoring the exotherm during foaming. The exotherm was monitored with a Martindale DT173 temperature probe placed at the center of the formulation (± 50 g of formulation placed in a plastic (PE) bottle of 8 cm height and 6 cm diameter. The initial temperature was measured after mixing TMPTC, the epoxide and hydrotalcite in a plastic vial. After adding and mixing the other components (KOH, water, amine according to procedure 4.3.3) at room temperature, the probe was placed laterally through the plastic vial at half height of the formulation and at the middle of the vial (center of the formulation). The probe was kept at this place without any perturbation until the end of measurement. Temperature was monitored every 30 seconds for 5 minutes and then every minute until 15 minutes. The start of the expansion was noted when the foam expanded from 2 mm above its initial height, and this time temperature is noted as the temperature to promote expansion. Results are summarized in Figure 3A

Monitoring the exotherm during the aminolysis or/and hydrolysis of TMPTC. The exotherm of both aminolysis and hydrolysis of TMPTC was monitored with a Martindale DT173 temperature probe along reaction time. The probe was introduced at the center of the formulation placed in a plastic (PE) bottle of 8 cm height and 6 cm diameter. For monitoring the aminolysis exotherm, TMPTC (28.9 g, 5CC = 200 mmol) was mixed with hydrotalcite (3 g) until dispersion of the clay in TMPTC. Then, XDA (10.3 g, NH_2 = 151 mmol) and TREN (3.18 g, NH_2 = 65 mmol) were added to TMPTC and stirred for 30 seconds until homogenization. The temperature was recorded for 15 min. For monitoring the hydrolysis exotherm, TMPTC (28.9 g, 5CC = 200 mmol) was first mixed with hydrotalcite (3g), Then KOH (1.4 g, 25 mmol) solubilized in water (0.9 g, 50 mmol) was added to the mixture and mixed for 30 sec. The temperature of the formulation was measured for 15 min. The exothermicity of both reactions (in a cascade fashion) was measured by adding to TMPTC (28.9 g, 5CC = 200 mmol) and hydrotalcite (3g), the amine mixture (XDA, 10.3 g, NH_2 = 151 mmol; and TREN, 3.18g, NH_2 = 65 mmol) and then KOH (1.4g, 25 mmol) solubilized in water (0.9g, 50 mmol). Results are summarized in Figure 3A.

Monitoring the exotherm during the aminolysis of TMPTE. The exotherm was monitored with a Martindale DT173 temperature probe introduced at the center of the formulation placed in a plastic (PE) bottle of 8 cm height and 6 cm diameter. TMPTE (29.1 g, epoxide = 289 mmol) was mixed with hydrotalcite (3 g). Then XDA (10.3 g, NH_2 = 151 mmol) and TREN (3.18 g, NH_2 = 65 mmol) were added. KOH (2 g, 36 mmol) solubilized in water (1.3 g, 72 mmol) was then added to the formulation. After homogenization by manual mixing, the temperature was monitored for 40 min. **It has to be noted that the aminolysis of TMPTE (without TMPTC) is highly exothermic and this experiment should be carried out with care as temperatures higher than 250 °C could be reached.** Results are summarized in Figure 3A. Experiment without KOH and water was also realized and present similar exotherm (F15, Figure S16)

Monitoring the aminolysis of neopentyl glycol dicyclic carbonate and neopentyl glycol diglycidyl ether Neopentyl glycol dicyclic carbonate (304 mg, 5CC = 2 mmol) was thermostatized at the given temperature (25, 40, 60, 80 or 100 °C) for 5 min. Benzylamine (214 mg, NH_2 = 2 mmol) was then added and the reaction medium was reacted under stirring for 15 min. The reaction was stopped by first adding 150 µL DCl (35%), then directly solubilized in DMSO-d_6 and stored at -20 °C. Neopentyl glycol diglycidyl ether (216 mg,

epoxide = 2 mmol) was thermostatized at the given temperature (25, 40, 60, 80 or 100 °C) for 5 min. Benzylamine (214 mg, NH_2 = 2 mmol) was then added to the medium that was then stirred for 15 min at target temperature. A sample was picked out, directly solubilized in DMSO-d_6 and stored at -20 °C to stop the reaction without adding any acid. For the two reactions, a control experiment was realized by mixing the reactants the same way but stopping the reaction directly after mixing (0 min) and storing the samples at – 20 °C. No reaction occurred under these storing conditions. All samples were analyzed by ^{1}H-NMR in DMSO-d_6. The results are summarized in Figure S10 and ^{1}H-NMR spectra are provided in supporting information (Figure S11 and S12).

Monitoring the hydrolysis of neopentyl glycol dicyclic carbonate and neopentyl glycol diglycidyl ether. Neopentyl glycol dicyclic carbonate (304 mg, 5CC = 2 mmol) was thermostatized at the given temperature (25, 40, 60, 80 or 100 °C) for 5 min. KOH (56 mg, 1 mmol) in water (36 mg, 2mmol) was then added and the reaction medium was reacted under stirring for 15 min. The reaction was stopped by first adding 150 µL DCl (35%), then directly solubilized in DMSO-d_6 and stored at -20 °C. Neopentyl glycol diglycidyl ether (216 mg, epoxide = 2 mmol) was thermostatized at the given temperature (25, 40, 60, 80 or 100 °C) for 5 min. KOH (56 mg, 1 mmol) in water (36 mg, 2mmol) was then added to the medium that was then stirred for 15 min at the target temperature. A sample was picked out, directly solubilized in DMSO-d_6 and stored at -20 °C to stop the reaction without adding any acid. For the two reactions, a control experiment was realized by mixing the reactants the same way but stopping the reaction directly after mixing (0 min) and storing the samples at – 20 °C. No reaction occurred under these storing conditions. All samples were analyzed by ^{1}H-NMR spectroscopy in DMSO-d_6. The results are summarized in Figure S10 and ^{1}H-NMR spectra are provided in supporting information Figure S13 and S14).

Results and discussion

Strategy to accelerate the foaming.

Foam fabrication through a self-foaming approach is governed by a complex interplay of key parameters. The blowing agent must be generated right on time when the visco-elastic characteristics of the formulation is optimal to enable the matrix expansion while avoiding the foam collapse. Up to now, the fastest water-induced self-blowing was obtained at 100 °C in 30 min, by mixing the pre-heated polyamine and poly(cyclic carbonate) at this temperature. These conditions served as a starting point to identify the main factors likely to accelerate the foaming. We selected one of our standard formulation (Formulation 1 (**F1**)) composed of a tris(cyclic carbonate) (TMPTC), *m*-xylylenediamine (XDA), water and KOH catalyst (5CC/NH_2/H_2O/KOH molar ratio of 1/0.75/0.25/0.125; where 5CC states for cyclic carbonate groups, and NH_2 for primary amines ones) (Figure 1A). A synthetic clay (hydrotalcite, 12 wt% *vs* TMPTC) was added to the formulation as it was demonstrated to improve the foam homogeneity.[27] This formulation generated enough CO_2 to expand the PHU matrix in less than 5 min when pre-heating all the components at 100 °C. However, the foam partly collapsed when removed from the oven after 5 min of curing, resulting in a high density uncrosslinked material (451 $kg.m^{-3}$, gel content (GC) = 0%; Figure 1B and Table S1, entry 3). Extending the curing time to 30 min at 100 °C enabled to produce a stable foam with a density of 275 $kg.m^{-3}$ and a gel content of 62% (Figure 1B and Table S1, entry 4). To get a detailed insight of the foaming process, rheology experiments were performed to determine the gel point (GP, defined as the crossover point between G' and G'') and the initial foam expansion (defined as the time to reach a 5% displacement of the rheological plates upon *in-situ* CO_2 release). Figure S1A shows that the gel point was reached in about 6 min with an initial foam expansion of 4.5 min, with low G' and G'' values. After 5 minutes, the foam was thus not crosslinked and the medium not viscous enough to efficiently trap CO_2, which explained its collapse after this short period of time. Over the next 25 minutes of curing, G' and G'' moduli increased slowly, though remaining low, indicating that the material was not highly crosslinked which is in line with the moderate gel content of 62%. This was further corroborated by FT-IR analyses of PHU foams fabricated after 5 and 30 min, with the typical carbonyl stretching band of the cyclic carbonate at 1790 cm^{-1} that decreased with the reaction time, however still largely present after 30 min (Figure 1C and Figure S2).

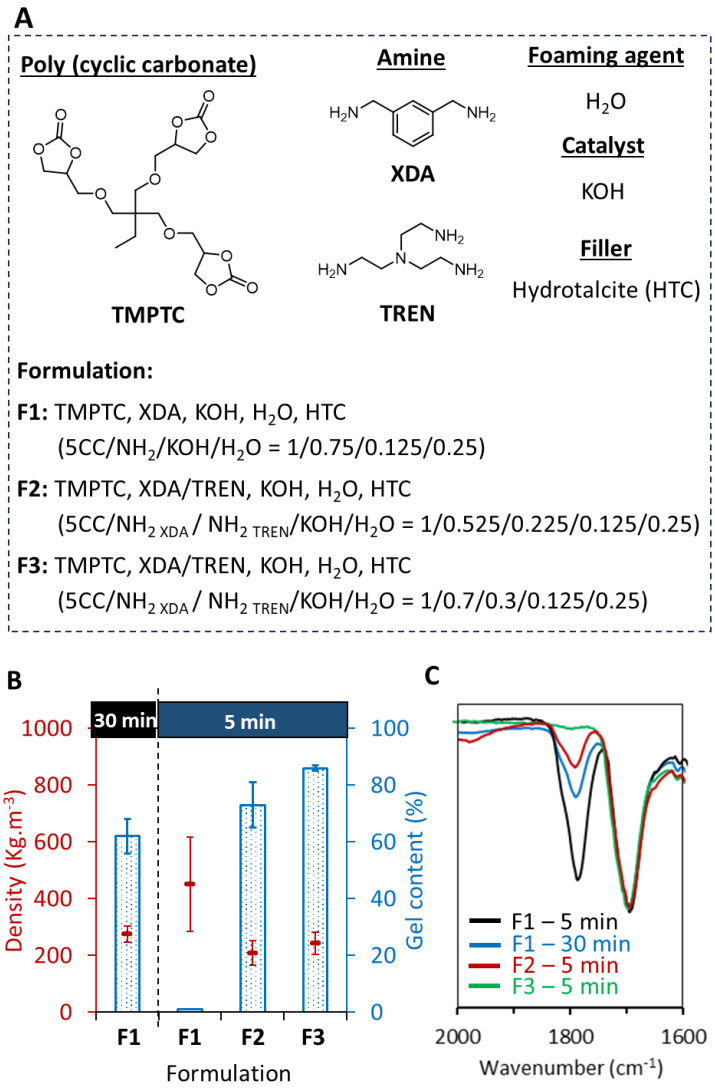

Figure 1. Water-induced fast self-foaming. A) Structure of the reagents and composition of the PHU formulations; B) Density and gel content of the foams synthesized from the different formulations after 30 and 5 minutes (Table S1); C) Infrared spectra (carbonyl region) of the different foams (normalized on the urethane carbonyl stretching band at 1690 cm^{-1} (full infrared spectra are presented in SI in Figure S2).

To deliver stable foams within 5 min, we thus had to address the inherent low reactivity of the PHU precursors to increase the crosslinking rate. We found inspiration from epoxy resins chemistry and PHU adhesives where tris(2-aminoethyl)amine (TREN) was used as a curing accelerator.[28] First, its trifunctional nature enabled to reach more rapidly the gel point. Beside, this polyamine displays an "aminoethyl amine"-type structure, known to enhance the primary amine group reactivity.[29,30] The foaming experiments were reproduced by using a mixture of XDA (NH_2 = 0.525 eq) and TREN (NH_2 = 0.225 eq) (Formulation 2 (**F2**), Figure 1A). Remarkably, both the gel and the foaming times were halved and reached within 2 minutes (Figure S1B) while the GC increased from 0 to 73% (Figure 1B). This enabled the formation of a stable foam with a density of 209 $kg.m^{-3}$ after 5 min

of curing at 100 °C. The benefit of adding TREN was also evidenced by FT-IR analysis, showing a higher cyclic carbonate consumption, but still incomplete (Figure 1C). By slightly increasing the amine content (1 eq. *vs* 5CC moieties instead of 0.75 eq.) while keeping constant the XDA/TREN molar ratio (Formulation 3 (**F3**), Figure 1A), quantitative consumption of the cyclic carbonate groups was reached in 5 min as attested by the complete disappearance of the carbonyl stretching band at 1790 cm^{-1} (Figure 1C, **F3**). GC was also increased to 86% (Figure 1B, **F3**), and G' and G'' moduli rapidly increased to reach high values (e.g. G' = 10^4 Pa after 5 min *vs* 10^2 -10^3 Pa for **F1** and **F2**, Figure S1C), in line with a rapid transition from viscous to solid state. Gel point and initial foaming time remained low (i.e. about 3 min), and the foam with a density of 242 $kg.m^{-3}$ did not collapse after 5 minutes. This optimal foam was characterized by a cell size of 0.42 ± 0.19 mm, slightly lower to the one observed for **F2** (0.78 ± 0.58 mm, Figure S3) as the result of the faster PHU crosslinking limiting the cells growth and coalescence (Figure 2C). In order to tune the rigidity of the foam, XDA was substituted by the more flexible aliphatic diamine EDR 148 (Figures 2A and 2B (**F4**)). As a result, the glass transition temperature (T_g) of the foam was decreased from 20.4 to -1.2 °C, while its density and GC remained similar after 5 min of reaction (comparison **F3** and **F4**, Figures 2B-C).

To align with the recent EU directives on sustainability goals of the plastic sector, petro-based TMPTC and XDA were respectively substituted by a tricyclic carbonate (GTC) derived from glycerol and biobased epichlorydrin, and hexamethylenediamine (HMDA) which the biobased production is now mastered at ton scale (Figure 2A).[31] The synthetic clay was replaced by a natural one (i.e. Cloisite Na). A flexible foam (T_g = -2.2 °C) with a high theoretical biobased content of 90 wt%, high GC (94%) and a density of 193 $kg.m^{-3}$ was produced. *We have to note here that we talk about "theoretical" biobased content when discussing about HMDA-based NIPU foams because the current HMDA feedstocks are petro-based.* The cell size was found higher (1.7 mm; Figures 2B-C) due to the use of a different filler (here, Cloisite Na instead of hydrotalcite). Indeed, the shape, size and exfoliation extent of the filler are known factors affecting the number and size of the cells.[23] To illustrate this statement, we replaced Cloisite Na by hydrotalcite in the formulation containing GTC (**F5**). Under identical foaming conditions, the foam morphology was different when the filler was changed (Figure S4). A rigid foam with a decent bio-based content of 72 wt% and free from aromatic compound was obtained by replacing HMDA by 1,3-bis(aminomethyl)cyclohexane (1,3-BAC, Figure 2A), while keeping similar properties than **F3** (T_g = 21.7 °C, d =167 $kg.m^{-3}$, GC = 91%, cell size = 1.9 mm) (Figures 2B-C). All these foams were producedin 5 min at 100 °C.

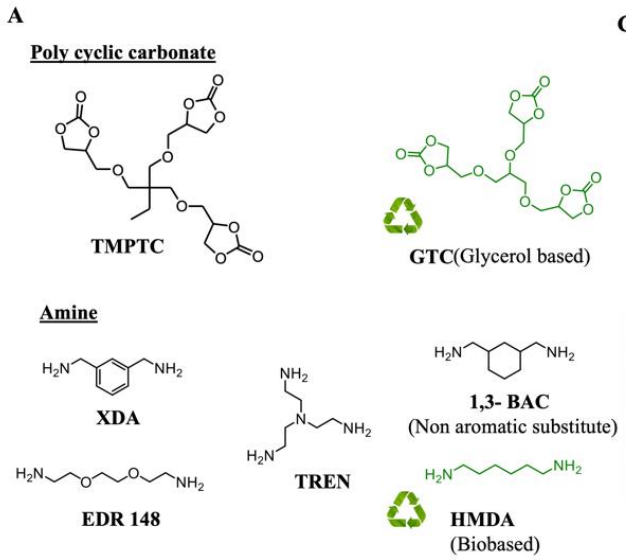

B

Form.	5CC	amine	Filler	d (kg.m^{-3})	GC (%)	T_g (°C)	Biobased content (%)
F3	TMPTC	XDA/TREN	HTC	242 ± 39	86 ± 1	20.4	0
F4	TMPTC	EDR/TREN	HTC	237 ± 56	89 ± 2	-1.2	0
F5	GTC	HMDA/TREN	CLOI	193 ± 42	94 ± 3	-2.2	90
F6	GTC	1,3-BAC/TREN	CLOI	167 ±17	91 ± 3	21.7	72

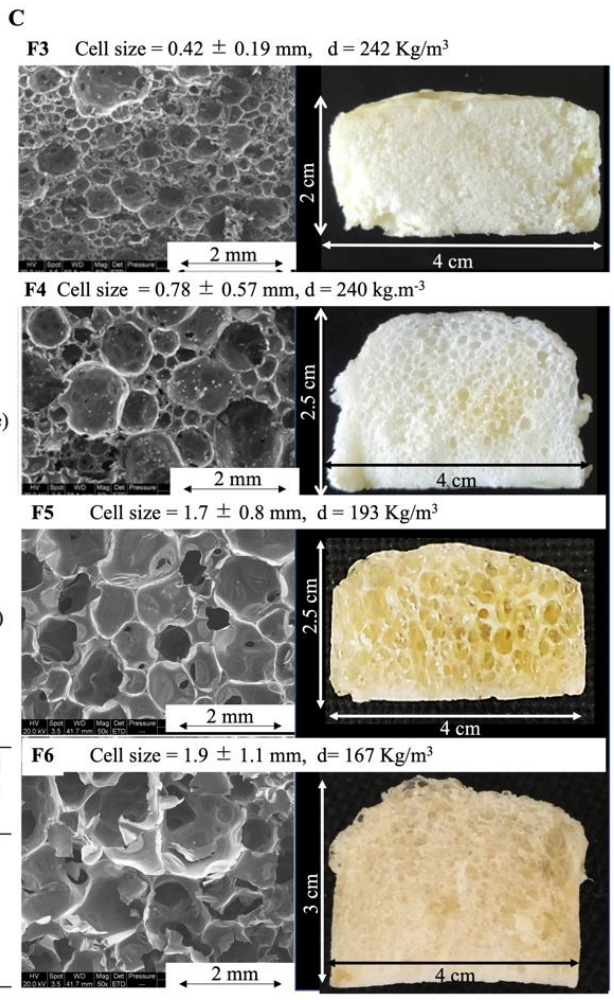

Figure 2. A) Components of PHU formulations used for the fast foaming procedure, including biobased monomers (in green). B) Formulations, properties and theoretical biobased content of PHU foams. C) SEM (left) and photography (right) of the different foams. Conditions: TMPTC or GTC (5CC = 1eq), XDA or EDR 148 or HMDA or 1,3-BAC (NH_2 = 0.7 eq), TREN (NH_2 = 0.3 eq), KOH (0.125 eq.), H_2O (0.25 eq.), 5 min at 100 °C. DSC thermograms are presented in Figure S5 to S8.

Strategy for fast foaming from room temperature formulations.

The above-mentioned results posed the foundations for the fast production of PHU foams, however at 100 °C. To unlock the necessary synthetic tools to realize this fast foaming from RT, we drew inspiration from the foaming of conventional PUs that benefits from the high exothermicity of the isocyanate/polyol reaction. The *in-situ* heat generation creates a "snowball effect" that rapidly raises the formulation temperature from RT to a range between 100 to 180 °C.[32,33] Applying the same strategy to self-blow PHU would require the reactions involved, i.e. the concomitant exothermic aminolysis and hydrolysis of cyclic carbonates, to release sufficient heat in a short time to raise the temperature from ambient to above the foaming temperature (around 85-90 °C). Starting from formulation **F3** at RT

(see Figure 1), we first investigated the exothermicity of the two concomitant reactions separately, i.e. the aminolysis of TMPTC by the mixture of XDA and TREN, and the hydrolysis of the cyclic carbonate (Figure 3A, blue curves). The aminolysis of TMPTC was exothermic and reached its maximal temperature of 64 °C after 7 min. This was also the case for the TMPTC hydrolysis, with a rapid (3 min.) temperature increase from RT to 40 °C when catalyzed by KOH. When carried out concomitantly, where both the amines and water/KOH were added together to TMPTC, the two reactions worked synergistically with an exotherm reaching 87 °C in 3 min (Figure 3A and 3C). However, this temperature was still insufficient to obtain PHU foams. Therefore, an additional "heat release promotor" was needed to impulse the foaming through cascade exotherms as illustrated in Figures 3A and 3C. We identified epoxides as ideal candidates since their aminolysis is known to create an important exotherm[34,35] that is correlated to the strain release of the cycle, further enhanced in epoxy resins by the rapid viscosity increase preventing efficient heat dissipation. Moreover, these precursors are compatible with the PHU chemistry, yet keeping the foaming process very simple while affording PHU/epoxide hybrids known to be robust materials with enhanced properties.[36–41] For the proof of concept, **F3** was modified by partly substituting TMPTC by its epoxy precursor, i.e. trimethylolpropane triglycidyl ether (TMPTE) (Figure 3A-B; see section 2 of ESI for details). The red curve of Figure 3A shows that epoxides and cyclic carbonates teamed up to significantly increase the reaction exotherm. A low epoxy loading of 0.25 eq (*vs* TMPTC) was already sufficient to initiate the fast foaming in about 3 min with a temperature increase within the core of the foam from RT to about 110 °C in less than 4 min (Figure 3A).

Further increase in the TMPTE content (from 0.33 to 3 eq *vs* TMPTC) enabled reaching much higher temperatures, up to 180 °C for the epoxy-rich formulation. Surprisingly, increasing the epoxide content delayed the exotherm (Figure 3A) as well as the time needed to start the foam expansion (from about 3 min with 0.25 eq TMPTE to 6 min with 3 eq; Figures 3A,D). To understand this delay, we evaluated the exothermicity of the pure epoxy resin formation by replacing all TMPTC by TMPTE. About 30 min were necessary to start observing a significant exotherm that became extremely high after 40 min (Figure 3A). These experiments suggested that the aminolysis and hydrolysis of 5CCs started at the initial stage of the process. These two reactions increased the temperature to the one required to initiate the highly exothermic epoxide aminolysis. These cascade exotherms rapidly raised the temperature above 100 °C, which induced the very fast foaming (Figure 3A and C). Whatever the TMPTE content, the maximum foam expansion was reached in a record timeframe (less than 1 min after the expansion started), and all foams were demolded directly after 15 min (time needed for the foams to sufficiently cool down). The initial foam expansion was observed at slightly lower temperature for the highest TMPTE content (e.g. 75 *vs* 90 °C for 3 *vs* 0.25 eq of TMPTE; Figure 3D), certainly due to the higher crosslinking degree of the formulation for high contents of epoxides that facilitated the trapping of the blowing agent. The exotherm and the foaming rate were thus easily controlled by the content of epoxide in the formulation (Figure 3D).

It is important to note that the presented foams were carried out on a 50 g scale. For a TMPTE/TMPTC molar ratio of 1/1, doubling the content of the formulation in the same foaming container (identical size and volume, see experimental section for details), a similar exotherm was observed and a foam with a similar gel content and density was obtained (Figure S9A,C). However, when decreasing the content of the formulation to 25 g

in the same container, the exothermicity was limited and provided a poor foaming (high density foam). This was due to the higher container/formulation volume ratio that favored heat dissipation and thus limited the exotherm. The similar trend was noted for a TMPTE/TMPTC molar ratio of 0.5 (Figure S9B,C).

As the two reactions involved in the polymer matrix construction (i.e. the aminolyses of the cyclic carbonate and epoxide) compete with each other as well as with the hydrolysis of the cyclic carbonate and possibly the epoxide, we performed additional analysis to demonstrate the hybrid nature of the foams, i.e. containing both urethane and amino alcohol linkages (Figure 3B). Model reactions (summarized in Figure S10) were performed on difunctional molecules and on a monofunctional amine to enable products characterizations by ^{1}H-NMR spectroscopy (Figure S11-S14). First, the aminolysis of model cyclic carbonate and epoxide (of the neopentyl glycol-type to mimic at best TMPTC and TMPTE) by benzylamine (to mimic XDA) were monitored by ^{1}H-NMR after 15 min of reaction at different temperatures (25, 40, 60, 80 and 100 °C; Figure S11 and S12). In line with previous exotherm evaluations, only the cyclic carbonate aminolysis occurred at 25 °C, while the aminolysis of the epoxide was initiated at a temperature higher than 60 °C (Figure S10). This experiment indicated that the aminolysis of cyclic carbonates was sufficiently fast to produce hydroxyurethanes even in the presence of epoxides. For higher temperatures, the two reactions occurred with the formation of both hydroxyurethane and amino alcohol functionalities, supporting the hybrid nature of our foams. FT-IR analysis of the foams supported the presence of urethane linkages by the characteristic carbonyl stretching band at 1700 cm^{-1} (Figure S15). The KOH catalyzed hydrolysis of the model cyclic carbonate also occurred at RT and was as fast as the aminolysis when the temperature reached 40 °C (Figure S10). On the other hand, the hydrolysis of the epoxide was very slow (almost not detectable) below 80 °C, and only 22% of the epoxide were hydrolyzed at 100 °C after 15 min of reaction. As both the aminolysis of the epoxide and the hydrolysis of the cyclic carbonate (that consumed water) were much faster than the hydrolysis of epoxide, this last reaction was less prone to significantly occur during the foaming process.

It must be noted that after synthesis, some residual cyclic carbonate groups were observed up to 0.5 eq of TMPTE (Figure S15). Full cyclic carbonate conversion was obtained for higher contents. This suggested that the higher exotherms generated when increasing the TMPTE content accelerated the consumption of the cyclic carbonates by aminolysis and hydrolysis. FT-IR spectra of TMPTE rich foams were very similar to the pure epoxy matrix (100 mol% TMPTE) but with the presence of the characteristic band of the urethane.

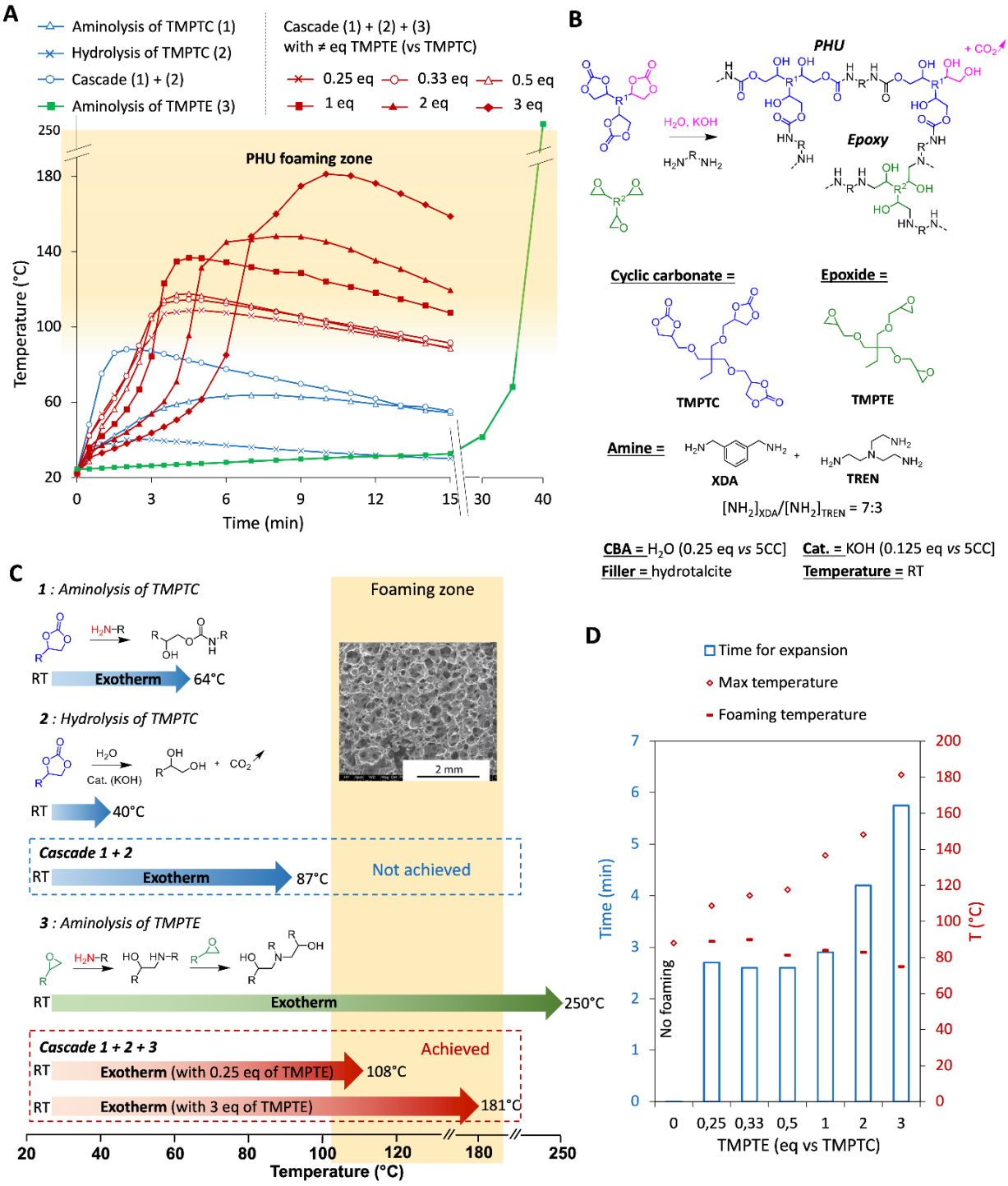

Figure 3. Reaction schemes and exotherms of the single reactions, as well as the cascade exotherms for self-foaming from RT formulations. A). Time evolution of the exotherms recorded for the aminolysis, hydrolysis, and concomitant hydrolysis and aminolysis of TMPTC (blue), aminolysis and hydrolysis of TMPTC in the presence of various contents of TMPTE (red), and aminolysis of TMPTE (green) (chemical structures for the reactions are provided in B)); B) Reaction scheme for the cascade reaction leading to

hybrid PHU foam, and structure of the reagents; C) Illustration of the individual reactions and cascade reactions with their corresponding exotherm; D) Time for expansion (time needed to start the foam expansion), foaming temperature (temperature when the foaming started) and maximum temperature reached during foaming (measured at the core of the foam). *Formulation compositions and conditions are detailed in supporting information in Tables S2-S3. Additional exotherms are added in Figure S16.*

As illustrated in Figure 4A, all hybrid foams displayed density values below 500 kg.m^{-3}. Clearly, the higher exotherm for high TMPTE contents favored the foam expansion. Indeed, the foam density progressively decreased with the epoxy content to reach about 200 kg.m^{-3} for the epoxy-rich formulations (1, 2 and 3 eq of TMPTE *vs* TMPTC). As for the conventional PU self-foaming process, a densification was also noted along the mold walls. This was reflected in low density values of the core of the foams ranging between 250 to 100 kg.m^{-3} (Figure 4A). The density gradient from the core to the foam border was attributed to the mold that constrained the foam expansion in one dimension and to the temperature dissipation along the mold walls. This was proven by simultaneously monitoring the temperature in the core and along the mold border for a formulation containing 1 eq of TMPTE. A maximal temperature of 81 °C was recorded at the border, while 136 °C was reached at the core (Figure S17). As discussed in the previous section, 81 °C was not sufficient for an efficient fast foam expansion, explaining this density gradient. All foams were rather similar with an open cell morphology and a mean cell size around 0.3 mm (Figure 4B and Table S4). However, the epoxy-rich formulations (TMPTE $\geq$ 2 eq vs TMPTC) provided heterogeneous foams with the core of the foams turning orange to brown due to the high temperature reached by the exotherm.

The higher exotherm induced with high TMPTE contents also provided a rapid stabilization/curing of the foam as reflected by FT-IR spectroscopy with the higher consumption of the cyclic carbonates (Figure S15) as well as an increase in the gel content from 80% for the pure PHU formulations up to 96% for the epoxy-rich hybrid foam (Figure 5A). Interestingly, we observed a difference of composition between the center and the outer part of the foams for samples prepared from epoxide reach formulations (TMPTE/TMPTC > 1). Indeed, in addition to the characteristic bands of hydroxyurethane (HU; carbonyl stretching at 1700 cm^{-1} and N-H band at 1530 cm^{-1}), the foam core also presented two new bands characteristic of urea at 1650 cm^{-1} (carbonyl stretching band) and 1550 cm^{-1} (N-H deformation vibration band) (Figure S18).[42] The appearance of urea was explained by the high temperature generated at the foam core for these epoxide-rich formulations. This observation is in line with works of Sardon et al that demonstrated that hydroxyurethane linkages of PHU were converted into urea ones at high temperature in the presence of a strong base catalyst. [42]

Foams made from TMPTE-poor formulations (0.25 to 1 eq of TMPTE) displayed a PHU-like behavior with T_g values around 21 °C (Figure 5B and Figure S19 to S23), rather close to the pure PHU material synthesized at 100 °C for 5 min (T_g = 20 °C, **F3** Figure 2B). In contrast, TMPTE-rich foams (2 to 3 eq of TMPTE) presented higher T_g values of 35 to 40 °C (Figure S24 and S25), close to the epoxy-matrix (Figure S26). The degradation temperature ($T_{d,5\%}$) for TMPTE-poor foams were evaluated between 226-237 °C while it increased by about 30 °C for the epoxide-rich ones (265 °C for 2 and 3 eq of TMPTE) yet

approaching the degradation temperature of the pure epoxy resin ($T_{d,5\%}$ = 295 °C) (Figure 5C, Table S4, Figure S27 to S34).

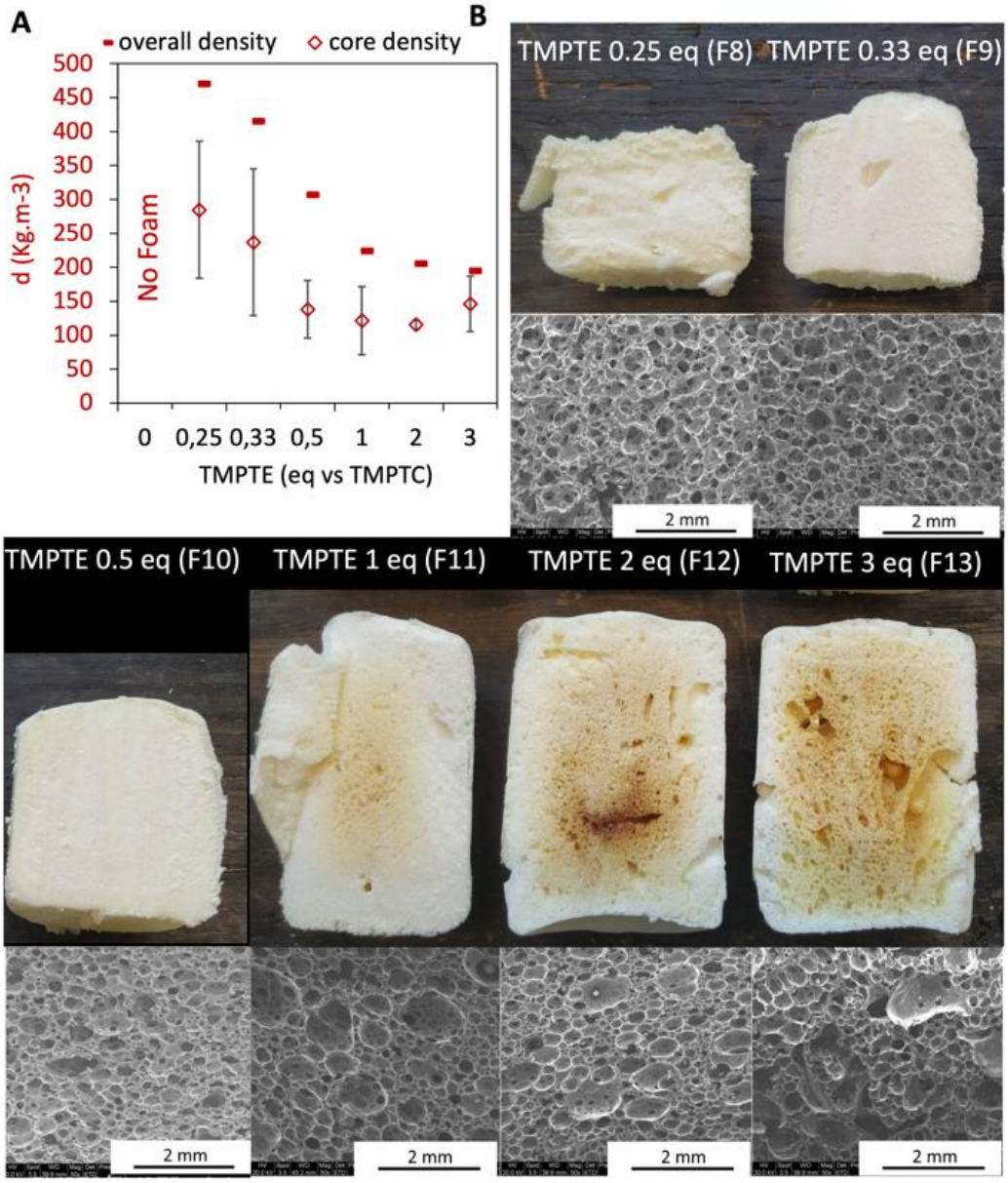

Figure 4. Density and morphology of self-blown hybrid foams made from RT formulations. A) Core and overall density of the different foams. B) Effect of the TMPTE content on the foam morphology. *The foam formulations are listed in Table S2, and the foam characteristics and properties are summarized in Table S4.*

Compression tests were performed on materials of similar densities, gel content and cell size. They were benchmarked with those realized on the pure PHU foams synthesized at 100 °C (**F3,** Figure 1). As expected, the compression modulus (E) increased with the TMPTE content in the formulation. For low TMPTE contents of 0.5 and 1 eq, the

compression modulus was estimated to 0.2 and 0.6 MPa, respectively, rather close to the one of the pure PHU foam (E = 0.3 MPa; Figure 5D). For the higher TMPTE contents of 2 and 3 eq, E was strongly increased to 3.7 and 4.7 MPa, respectively. Although direct comparison of all samples could not be done due to slight differences in the morphology and densities of the tested foams, the main trend was that hybrid foams with an epoxy content up to 1 eq resembled to the pure PHU foam. For higher TMPTE contents, the foams became more rigid, in line with a higher crosslinking density imparted by the epoxy network.

Although utilized in a plethora of material applications (e.g. for epoxy resin fabrication) [28,43], TREN is acutely toxic, a skin sensitizer, and long-term aquatic hazard (see product safety data sheet) and is thus certainly not the best candidate for designing greener materials. However, it was used in a low amount in our formulations (about 5 wt%). To go a step further, we investigated the possibility to avoid its use. For that purpose, we followed the exotherm of the optimal formulation (i.e. with a TMPTC/TMPTE molar ratio of 1) without TREN and the results are depicted in Figure S35. The exotherm and the foaming were delayed in the absence of TREN, from 3 to 6 min (Figure S35B). Despite a delayed foaming, a foam with a similar density and T_g value than foam **F11** (prepared with TREN) was obtained, and a full conversion of 5CC was also noticed. A lower gel content of 80% (*vs* 98%) was however obtained, as expected when substituting a triamine by a diamine. This experiment demonstrated that TREN was not mandatory for the foaming under these conditions but slightly delayed the process and significantly decreased the gel content. Future works should focus on utilizing greener polyamines.

The versatility of the fast PHU self-foaming technology was then proven in concept by designing flexible and rigid foams (Figure 6, Table S5 for formulations). For reactive formulations made of 1 eq of TMPTE, the replacement of XDA by its hydrogenated cycloaliphatic variant (1,3-BAC) or the aliphatic diamine (EDR 148) delivered foams with overall densities between 200 and 300 $kg.m^{-3}$ and high gel contents (> 94%) (Figure 6A-C, Table S6). Monitoring the formulation temperature with the foaming time evidenced the important exotherm, with a maximum temperature of about 140 °C observed in the three cases after 3 to 5 minutes (Figure S36). All foams were easily demolded after 15 min, and were characterized by T_g values of 26, 45 and 2 °C for the XDA-, 1,3-BAC- and EDR 148-based foams, respectively (Figure 6C). Other epoxides were also utilized such as commercially available diepoxides (e.g. aromatic bisphenol A diglycidyl ether (DER 332) or butanediol diglycidyl ether (BDGE); Figure 6A). By replacing TMPTE by DER 332 or BDGE, demoldable hybrid foams were also recovered after 15 min with densities of 200 to 300 $kg.m^{-3}$, high gel contents (about 90%) and T_g values of 47 and 16 °C associated to compressive modulus of 1.9 MPa and 0.017 MPa (Table S6), respectively. As illustrated in Figure S37, similar exotherms and short times to expansion (2 to 3.5 min) were noted.

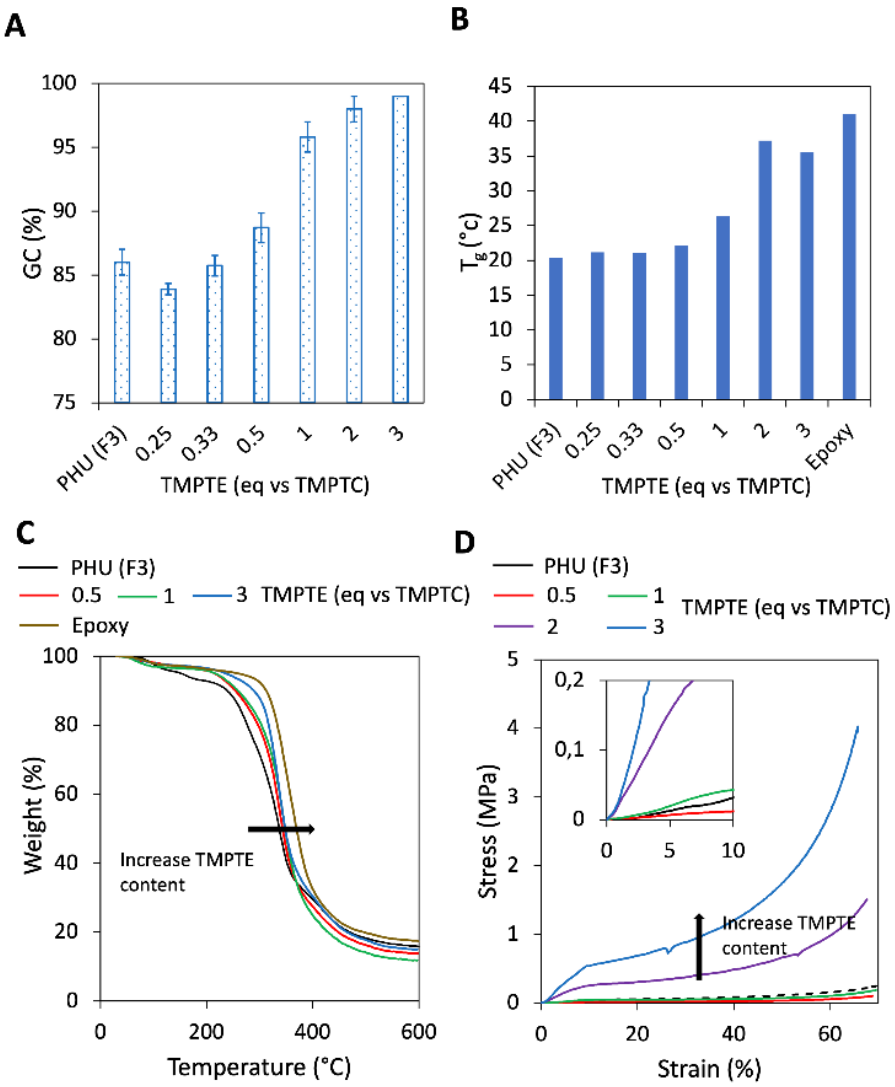

Figure 5. Properties of the hybrid foams synthesized from RT formulations. A) Gel content; B) Glass transition temperature (DSC thermograms are presented in Figures S13-S20); C) Selected thermograms of the different foams (all thermograms are provided in Figure S21 to S28); D) Strain/stress curves for some selected foams. *The different formulations for preparing the different foams are listed in Table S2 and properties are presented in Table S4.*

To illustrate the potential of the process for producing more sustainable foams of high bio-based content (70 to theoretically 90 wt%), the petro-based cyclic carbonate (TMPTC) and epoxide (TMPTE) were substituted for glycerol-based alternatives (GTC and GTE, respectively; Figure 6B), and the synthetic filler was replaced by a natural one (Cloisite Na). With 1,3-BAC as the diamine and 1 eq of GTE (*vs* GTC, see Table S5, exotherms presented in Figure S38), a highly cross-linked foam (T_g = 35.4 °C and GC = 98%, compressive modulus = 0.032 MPa) with an homogeneous pore size distribution (cell size = 0.85 ± 0.22 mm; Figure 6D, **F20**), an overall density of 189 kg.m^{-3} (core density of 117 kg.m^{-3}) and a bio-based content of 68 wt% was obtained (Figure 6C). By substituting 1,3-

BAC for HMDA, and 0.5 eq of GTE (*vs* GTC, see Table S5) a more flexible crosslinked foam (T_g = -7 °C and GC = 98%, compressive modulus = 0.0067 MPa) was produced with a theoretical bio-based content as high as 90 wt%. This foam was highly homogeneous with very similar density than the previous one (overall density = 212 kg.m^{-3}; core density = 100 kg.m^{-3}; cell size = 0.92 ± 0.19 mm ;Figure 6C-D, **F21**). The foaming of this formulation **F21** was very fast (about 1.5 min) and is shown in the video provided in ESI. All compressive curves are presented in Figure S39.

Importantly, the pendant hydroxyl groups of this hybrid flexible bio-based foam **F21** were exploited to repurpose/upcycle it into film by a combination of transcarbamoylation and dissociative hydroxyurethane reactions. Such strategy was exploited for recycling PHU foams, [26,44–46] but also commercial PU foams.[47,48] By pressing the crosslinked hybrid bio-based foam **F21** under the same conditions than those previously reported for other self-blown PHU foams (160 °C, 2 T, 2 h),[24,27] a thin homogeneous polymer film (width = 0.19 mm, Figure 6E) with a modulus of 1.66 MPa and a strain at break of 14% was obtained (Figure 6E1). Neither the T_g of the obtained film (-3 °C for the film *vs* -7 °C for the foam) nor the comparative infrared analysis (Figure 6E1) indicated a significant change in the chemical structure during this first foam reprocessing.

We have then studied the possibility to reprocess again the so-formed film. The experiment was carried out under identical conditions than for reprocessing the foam by hot pressing (160 °C, 2h, pressure of 2T, after cutting the sample into small pieces). However, an inhomogeneous brittle film with cracks and defects was obtained (Figure S46A). A stress relaxation experiment carried out at 160 °C on the film obtained from the first foam reprocessing showed that the stress and modulus of the polymer film were constant over the first 100 seconds (Figure S46B). However, we observed an increase in their values after this period of time, with an equilibration appearing after more than 3 h. The FTIR analysis performed on the film before and after the second reprocessing, as well as after the long (5 h) stress relaxation experiment at 160 °C, showed some changes in the chemical nature of the film. A significant increase in the intensity of the band at 1650 cm^{-1} was indeed observed during long treatments at this temperature (Figure S46C). Importantly, the same behavior was observed when reprocessing the foam **F5** (Figure 2) that was obtained without any epoxide in the formulation (Figure S46D). The lack of reprocessability of the film obtained from foam **F21** for the second cycle was thus not linked to its hybrid structure. The band observed at 1650 cm^{-1} might come from some urea formation, known to appear in this temperature range.[42]

Although deeper investigations are needed to understand the whole repurposing process, to optimize it to decrease both the processing temperature and time, and thus to limit the occurrence of side reactions observed during multiple recycling cycles, these preliminary experiments illustrated that the hybrid nature of the foam did not prevent the foam reprocessability/upcycling into a polymer film.

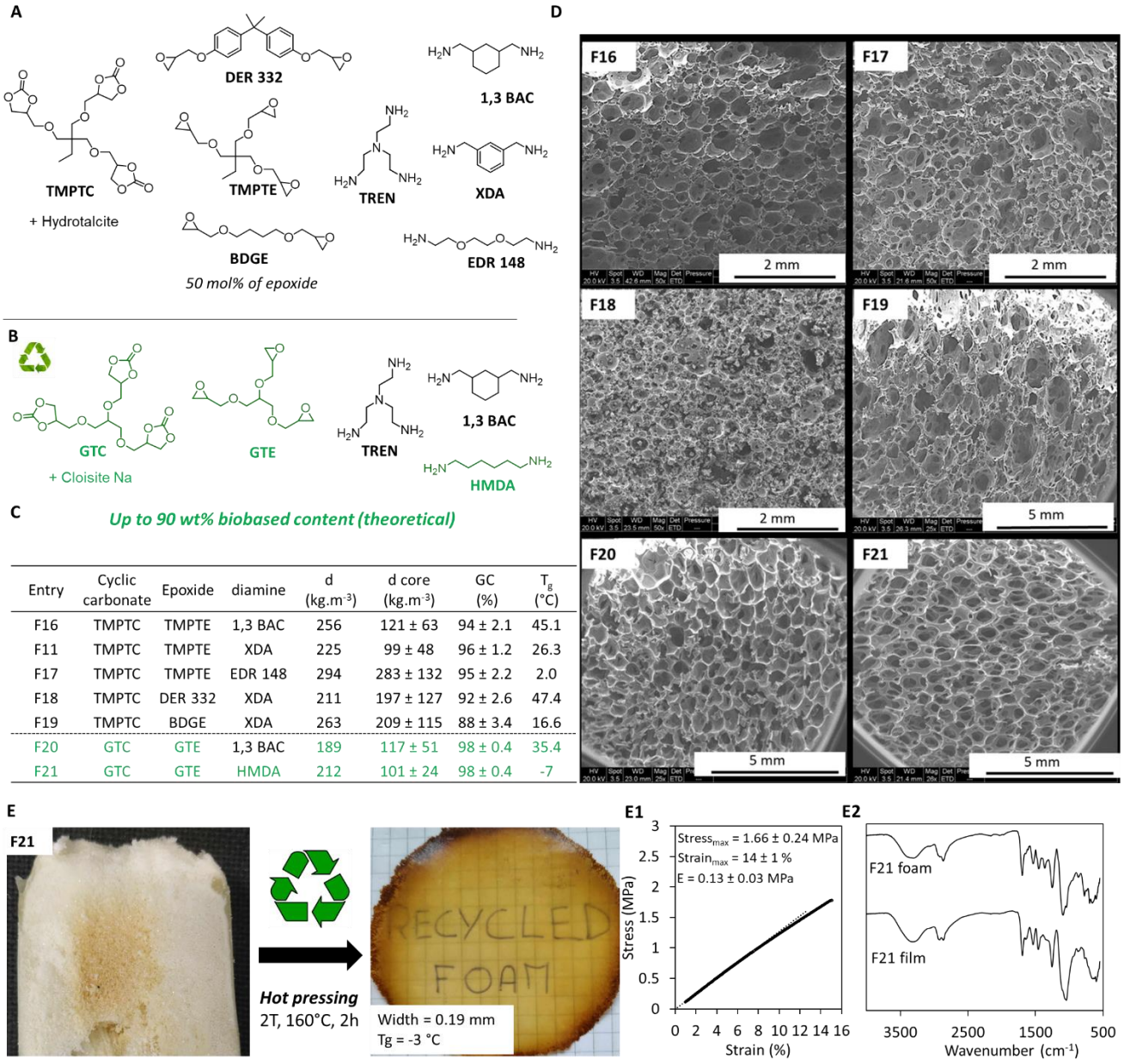

Entry	Cyclic carbonate	Epoxide	diamine	d (kg.m^{-3})	d core (kg.m^{-3})	GC (%)	T_g (°C)
F16	TMPTC	TMPTE	1,3 BAC	256	121 ± 63	94 ± 2.1	45.1
F11	TMPTC	TMPTE	XDA	225	99 ± 48	96 ± 1.2	26.3
F17	TMPTC	TMPTE	EDR 148	294	283 ± 132	95 ± 2.2	2.0
F18	TMPTC	DER 332	XDA	211	197 ± 127	92 ± 2.6	47.4
F19	TMPTC	BDGE	XDA	263	209 ± 115	88 ± 3.4	16.6
F20	GTC	GTE	1,3 BAC	189	117 ± 51	98 ± 0.4	35.4
F21	GTC	GTE	HMDA	212	101 ± 24	98 ± 0.4	-7

Figure 6. Scope of PHU hybrid foams prepared from RT formulations, including foams of high biobased contents. A) List of monomers used for producing PHU hybrid foams from RT formulations; B) Structure of the monomers used for preparing foams with high theoretical biobased content (68 wt%), formulation **F20**; 90 wt%, formulation **F21**); C) Formulations and foams properties (DSC thermograms are presented in Figure S40 to S45); D) SEM images of the different foams; E) Recycling of the biobased foam **F21** into film by hot pressing: (E1) tensile properties of the film, and (E2) comparison of FT-IR spectra of the foam and the reprocessed film. *Foams formulations and properties are depicted in Tables S5 and S6.*

Conclusions

Water-induced self-blown non-isocyanate polyurethane (NIPU) foams are promising sustainable alternatives to conventional isocyanate-based polyurethane foams. However, their production was still slow (i.e. 30 min at 100 °C), far away from 2-10 minutes from room temperature formulations required for many industrial foaming processes. Herein, we identified the reasons for these slow processes, and unlocked strategies to tackle them, allowing the production of NIPU foams in short time frames (2-10 minutes) from RT formulations. Our studies showed that, besides rapidly generating the blowing agent (CO_2), the crosslinking of the polymer matrix had to be strongly accelerated to properly expand the matrix while avoiding its collapse. This was achieved by adding a highly reactive triamine of the "aminoethyl amine"-type to the solvent-free formulation. To enable the foaming from RT formulation, we leveraged cascade exothermic reactions enabling to rapidly raise the formulation temperature to trigger the foaming. Indeed, while the moderately exothermic concomitant aminolysis and hydrolysis of the cyclic carbonate failed to trigger the foaming, they enabled to initiate the fast aminolysis of an epoxide added to the formulation. In turn, this highly exothermic reaction accelerated the foaming process by strongly raising the temperature and by increasing the matrix crosslinking degree. Hybrid PHU foams were thus obtained in minutes timeframes, whose properties were easily tuned from rigid to flexible foams by adapting the nature of the comonomers, as well as the content of epoxide. By selecting bio-based monomers, homogeneous hybrid PHU foams of high theoretical bio-content (up to 90 wt%) were rapidly produced for the first time from RT formulations. Moreover, their repurposing/recycling into polymer films was validated by simple hot-pressing without any noticeable degradation. Although hybrid PHU foams were obtained by this foaming process based on cascade exotherms, the retrofit of the PU foam industry is now potentially possible for producing more sustainable and recyclable foams. As the process is highly versatile and simple for manufacturing foams of various properties in record time frames, it is of great promise to meet the vast foam market demand.

Associate content

Supporting information provides monomer synthesis procedures and characterizations, infrared spectra, DSC and TGA thermograms, exotherms of foaming reaction and ^{1}H NMR spectra of model reactions. The fast foaming of formulation **F21** is also shown in the video provided in ESI. This material is available free of charge via the Internet at http://pubs.acs.org."

A preprint of this article appeared on ChemRxiv at DOI: 10.26434/chemrxiv-2023-t48bf.

Conflict of interest

The authors declare no competing financial interest.

Acknowledgements

The authors thank the Region Wallonne for funding the Win2Wal project "ECOFOAM" (convention 2010130). They also thank the company NMC sa (Belgium) for their support in this research. The authors are very grateful to Grégory Cartigny for technical assistance

in the preparation of the formulations and the foams. C.D. is FNRS Research Director and thanks the "Fonds de la Recherche Scientifique (F.R.S.-FNRS) for funding. Part of this work was realized to provide preliminary data supporting the feasibility of the WEL-T Advanced Grant proposal submitted by C.D. C.D. is particularly grateful to the Region Wallonne for having recently granted this project (FRFS-WEL-T; project "CHEMISTRY", convention WEL-T-CR-2023 A – 02). The authors have patented the technology (WO 2023/104362A1).

References

(1) MarketandMarkets, www.marketsandmarkets.com, Polyurethane Foam Market by Type (Rigid Foam, Flexible Foam, Spray Foam), End-Use Industry (Building & Construction, Bedding & Furniture, Automotive, Electronics, Footwear, Packaging), and Region – Global Forecast to 2028, https://www.marketsandmarkets.com/Market-Reports/polyurethane-foams-market-1251.html, September, **2023**

(2) Akindoyo, J. O.; Beg, M. D. H.; Ghazali, S.; Islam, M. R.; Jeyaratnam, N.; Yuvaraj, A. R. Polyurethane Types, Synthesis and Applications-a Review. RSC Adv **2016**, 6 (115), 114453–114482. https://doi.org/10.1039/c6ra14525f.

(3) Engels, H.-W.; Pirkl, H.-G.; Albers, R.; Albach, R. W.; Krause, J.; Hoffmann, A.; Casselmann, H.; Dormish, J. Polyurethanes: Versatile Materials and Sustainable Problem Solvers for Today's Challenges. Angewandte Chemie International Edition **2013**, 52 (36), 9422–9441. https://doi.org/10.1002/anie.201302766.

(4) IMARC group, www.imarcgroup.com, Polyurethane (PU) Foam Market: Global Industry Trends, Share, Size, Growth, Opportunity and Forecast 2023-2028, https://www.imarcgroup.com/polyurethane-foam-market. **2022**

(5) Peyrton, J.; Avérous, L. Structure-Properties Relationships of Cellular Materials from Biobased Polyurethane Foams. Materials Science and Engineering: R: Reports **2021**, 145, 100608. https://doi.org/https://doi.org/10.1016/j.mser.2021.100608.

(6) Karol, M. H.; Kramarik, J. A. Phenyl Isocyanate Is a Potent Chemical Sensitizer. Toxicol Lett **1996**, 89 (2), 139–146. https://doi.org/https://doi.org/10.1016/S0378-4274(96)03798-8.

(7) Bello, D.; Herrick, C. A.; Smith, T. J.; Woskie, S. R.; Streicher, R. P.; Cullen, M. R.; Liu, Y.; Redlich, C. A. Skin Exposure to Isocyanates: Reasons for Concern. Environ Health Perspect **2007**, 115 (3), 328–335. https://doi.org/10.1289/ehp.9557.

(8) S.Merenyi. REACH: Regulation (EC) No 1907/2006: Consolidated Version (June 2012) with an Introduction and Future Prospects Regarding the Area of Chemicals Legislation (Vol. 2). GRIN Verlag.

(9) European Commisson. Communication from the Commission to the European Parliament and the Council, Sustainable Carbon Cycles; Brussels, 2021. https://climate.ec.europa.eu/system/files/2021-12/com_2021_800_en_0.pdf (accessed 2023-09-28).

(10) Kathalewar, M. S.; Joshi, P. B.; Sabnis, A. S.; Malshe, V. C. Non-Isocyanate Polyurethanes: From Chemistry to Applications. RSC Adv **2013**, 3 (13), 4110. https://doi.org/10.1039/c2ra21938g.

(11) Cornille, A.; Auvergne, R.; Figovsky, O.; Boutevin, B.; Caillol, S. A Perspective Approach to Sustainable Routes for Non-Isocyanate Polyurethanes. Eur Polym J **2017**, 87, 535–552. https://doi.org/10.1016/j.eurpolymj.2016.11.027.

(12) Maisonneuve, L.; Lamarzelle, O.; Rix, E.; Grau, E.; Cramail, H. Isocyanate-Free Routes to Polyurethanes and Poly(Hydroxy Urethane)s. Chem Rev **2015**, 115 (22), 12407–12439. https://doi.org/10.1021/acs.chemrev.5b00355.

(13) Blattmann, H.; Lauth, M.; Mülhaupt, R. Flexible and Bio-Based Nonisocyanate Polyurethane (NIPU) Foams. Macromol Mater Eng **2016**, 301 (8), 944–952. https://doi.org/10.1002/mame.201600141.

(14) Grignard, B.; Thomassin, J.-M.; Gennen, S.; Poussard, L.; Bonnaud, L.; Raquez, J.-M.; Dubois, P.; Tran, M.-P.; Park, C. B.; Jerome, C.; Detrembleur, C. CO2-Blown Microcellular Non-Isocyanate Polyurethane (NIPU) Foams: From Bio- and CO2-Sourced Monomers to Potentially Thermal Insulating Materials. Green Chem. **2016**, 18 (7), 2206–2215. https://doi.org/10.1039/C5GC02723C.

(15) Dong, T.; Dheressa, E.; Wiatrowski, M.; Pereira, A. P.; Zeller, A.; Laurens, L. M. L.; Pienkos, P. T. Assessment of Plant and Microalgal Oil-Derived Nonisocyanate Polyurethane Products for Potential Commercialization. ACS Sustain Chem Eng **2021**, 9 (38), 12858–12869. https://doi.org/10.1021/acssuschemeng.1c03653.

(16) Amezúa-Arranz, C.; Santiago-Calvo, M.; Rodríguez-Pérez, M.-Á. A New Synthesis Route to Produce Isocyanate-Free Polyurethane Foams. Eur Polym J **2023**, 197, 112366. https://doi.org/https://doi.org/10.1016/j.eurpolymj.2023.112366.

(17) Cornille, A.; Dworakowska, S.; Bogdal, D.; Boutevin, B.; Caillol, S. A New Way of Creating Cellular Polyurethane Materials: NIPU Foams. Eur Polym J **2015**, 66, 129–138. https://doi.org/https://doi.org/10.1016/j.eurpolymj.2015.01.034.

(18) Cornille, A.; Guillet, C.; Benyahya, S.; Negrell, C.; Boutevin, B.; Caillol, S. Room Temperature Flexible Isocyanate-Free Polyurethane Foams. Eur Polym J **2016**, 84, 873–888. https://doi.org/https://doi.org/10.1016/j.eurpolymj.2016.05.032.

(19) Coste, G.; Berne, D.; Ladmiral, V.; Negrell, C.; Caillol, S. Non-Isocyanate Polyurethane Foams Based on Six-Membered Cyclic Carbonates. Eur Polym J **2022**, 176, 111392. https://doi.org/https://doi.org/10.1016/j.eurpolymj.2022.111392.

(20) Coste, G.; Denis, M.; Sonnier, R.; Caillol, S.; Negrell, C. Synthesis of Reactive Phosphorus-Based Carbonate for Flame Retardant Polyhydroxyurethane Foams. Polym Degrad Stab **2022**, 202, 110031. https://doi.org/https://doi.org/10.1016/j.polymdegradstab.2022.110031.

(21) Choong, P. Sen; Hui, Y. L. E.; Lim, C. C. CO2-Blown Nonisocyanate Polyurethane Foams. ACS Macro Lett **2023**, 12 (8), 1094–1099. https://doi.org/10.1021/acsmacrolett.3c00334.

(22) Clark, J. H.; Farmer, T. J.; Ingram, I. D. V; Lie, Y.; North, M. Renewable Self-Blowing Non-Isocyanate Polyurethane Foams from Lysine and Sorbitol. European J Org Chem **2018**, 2018 (31), 4265–4271. https://doi.org/10.1002/ejoc.201800665.

(23) Monie, F.; Grignard, B.; Thomassin, J.-M.; Mereau, R.; Tassaing, T.; Jerome, C.; Detrembleur, C. Chemo- and Regioselective Additions of Nucleophiles to Cyclic

Carbonates for the Preparation of Self-Blowing Non-Isocyanate Polyurethane Foams. Angewandte Chemie International Edition **2020**, 59 (39), 17033–17041. https://doi.org/https://doi.org/10.1002/anie.202006267.

(24) Monie, F.; Grignard, B.; Detrembleur, C. Divergent Aminolysis Approach for Constructing Recyclable Self-Blown Nonisocyanate Polyurethane Foams. ACS Macro Lett **2022**, 11 (2), 236–242. https://doi.org/10.1021/acsmacrolett.1c00793.

(25) Coste, G.; Negrell, C.; Caillol, S. Cascade (Dithio)Carbonate Ring Opening Reactions for Self-Blowing Polyhydroxythiourethane Foams. Macromol Rapid Commun **2022**, 43 (13), 2100833. https://doi.org/https://doi.org/10.1002/marc.202100833.

(26) Purwanto, N. S.; Chen, Y.; Wang, T.; Torkelson, J. M. Rapidly Synthesized, Self-Blowing, Non-Isocyanate Polyurethane Network Foams with Reprocessing to Bulk Networks via Hydroxyurethane Dynamic Chemistry. Polymer (Guildf) **2023**, 272, 125858. https://doi.org/https://doi.org/10.1016/j.polymer.2023.125858.

(27) Bourguignon, M.; Grignard, B.; Detrembleur, C. Water-Induced Self-Blown Non-Isocyanate Polyurethane Foams. Angewandte Chemie International Edition **2022**, 61 (51), e202213422. https://doi.org/https://doi.org/10.1002/anie.202213422.

(28) Capar, Ö.; Tabatabai, M.; Klee, J. E.; Worm, M.; Hartmann, L.; Ritter, H. Fast Curing of Polyhydroxyurethanes via Ring Opening Polyaddition of Low Viscosity Cyclic Carbonates and Amines. Polym. Chem. **2020**, 11 (43), 6964–6970. https://doi.org/10.1039/D0PY01172J.

(29) Diakoumakos, C. D.; Kotzev, D. L. Non-Isocyanate-Based Polyurethanes Derived upon the Reaction of Amines with Cyclocarbonate Resins. Macromol Symp **2004**, 216, 37–46. https://doi.org/10.1002/masy.200451205.

(30) Hernández, A.; Houck, H. A.; Elizalde, F.; Guerre, M.; Sardon, H.; Du Prez, F. E. Internal Catalysis on the Opposite Side of the Fence in Non-Isocyanate Polyurethane Covalent Adaptable Networks. Eur Polym J **2022**, 168, 111100. https://doi.org/https://doi.org/10.1016/j.eurpolymj.2022.111100.

(31) Rothbarth, F.; Stockhausen, T.; Mann, C.; Grubaugh, K.; Covestro and Genomatica produce important chemical raw material using biotechnology, Covestro Press, https://www.covestro.com/press/covestro-and-genomatica-produce-important-chemical-raw-material-using-biotechnology/. January 19th, **2022**

(32) Van Gheluwe, P.; Leroux, J. Sequential Nature of the Exothermic Reactions Leading to the Formation of Flexible Polyurethane Foams. J Appl Polym Sci **1983**, 28 (6), 2053–2067. https://doi.org/https://doi.org/10.1002/app.1983.070280618.

(33) Xin, H.; Zhang, P.; Zhang, B.; Zhu, Y.; Wu, J.; Lin, Y.; Qi, X.; Liu, C.; Wang, H.; Wang, D.; Lin, Z. Polyurethane Exothermic Polymerization and Phase Change Material Thermal Delay Matching: An Approach to Reducing Fire Risks in Mining Polymer Materials. ACS Appl Polym Mater **2023**. https://doi.org/10.1021/acsapm.3c01125.

(34) Ran, Z.; Liu, X.; Jiang, X.; Wu, Y.; Liao, H. Study on Curing Kinetics of Epoxy-Amine to Reduce Temperature Caused by the Exothermic Reaction. Thermochim Acta **2020**, 692, 178735. https://doi.org/https://doi.org/10.1016/j.tca.2020.178735.

(35) Marsella, J. A.; Starner, W. E. Acceleration of Amine/Epoxy Reactions with N-Methyl Secondary Amines. J Polym Sci A Polym Chem **2000**, 38 (5), 921–930. https://doi.org/https://doi.org/10.1002/(SICI)1099-0518(20000301)38:5<921::AID-POLA17>3.0.CO;2-P.

(36) Figovsky, O.; Shapovalov, L.; Birukova, O.; Leykin, A. Modification of Epoxy Adhesives by Hydroxyurethane Components on the Basis of Renewable Raw Materials. Polymer Science Series D **2013**, 6 (4), 271–274. https://doi.org/10.1134/S1995421213040047.

(37) Lambeth, R. H.; Rizvi, A. Mechanical and Adhesive Properties of Hybrid Epoxy-Polyhydroxyurethane Network Polymers. Polymer (Guildf) **2019**, 183, 121881. https://doi.org/https://doi.org/10.1016/j.polymer.2019.121881.

(38) Anitha, S.; Vijayalakshmi, K. P.; Unnikrishnan, G.; Kumar, K. S. S. CO2 Derived Hydrogen Bonding Spacer: Enhanced Toughness{,} Transparency{,} Elongation and Non-Covalent Interactions in Epoxy-Hydroxyurethane Networks. J. Mater. Chem. A **2017**, 5 (46), 24299–24313. https://doi.org/10.1039/C7TA08243F.

(39) Helbling, P.; Hermant, F.; Petit, M.; Tassaing, T.; Vidil, T.; Cramail, H. Unveiling the Reactivity of Epoxides in Carbonated Epoxidized Soybean Oil and Application in the Stepwise Synthesis of Hybrid Poly(Hydroxyurethane) Thermosets. Polym. Chem. **2023**, 14 (4), 500–513. https://doi.org/10.1039/D2PY01318E.

(40) Gomez-Lopez, A.; Elizalde, F.; Calvo, I.; Sardon, H. Trends in Non-Isocyanate Polyurethane (NIPU) Development. Chem. Commun. **2021**, 57 (92), 12254–12265. https://doi.org/10.1039/D1CC05009E.

(41) Ecochard, Y.; Caillol, S. Hybrid Polyhydroxyurethanes: How to Overcome Limitations and Reach Cutting Edge Properties? Eur Polym J **2020**, 137, 109915. https://doi.org/https://doi.org/10.1016/j.eurpolymj.2020.109915.

(42) Bossion, A.; Aguirresarobe, R. H.; Irusta, L.; Taton, D.; Cramail, H.; Grau, E.; Mecerreyes, D.; Su, C.; Liu, G.; Müller, A. J.; Sardon, H. Unexpected Synthesis of Segmented Poly(Hydroxyurea–Urethane)s from Dicyclic Carbonates and Diamines by Organocatalysis. Macromolecules **2018**, 51 (15), 5556–5566. https://doi.org/10.1021/acs.macromol.8b00731.

(43) Spiesschaert, Y.; Guerre, M.; De Baere, I.; Van Paepegem, W.; Winne, J. M.; Du Prez, F. E. Dynamic Curing Agents for Amine-Hardened Epoxy Vitrimers with Short (Re)Processing Times. Macromolecules **2020**, 53 (7), 2485–2495. https://doi.org/10.1021/acs.macromol.9b02526.

(44) Fortman, D. J.; Brutman, J. P.; Cramer, C. J.; Hillmyer, M. A.; Dichtel, W. R. Mechanically Activated, Catalyst-Free Polyhydroxyurethane Vitrimers. J Am Chem Soc **2015**, 137 (44), 14019–14022. https://doi.org/10.1021/jacs.5b08084.

(45) Chen, X.; Li, L.; Jin, K.; Torkelson, J. M. Reprocessable Polyhydroxyurethane Networks Exhibiting Full Property Recovery and Concurrent Associative and Dissociative Dynamic Chemistry: Via Transcarbamoylation and Reversible Cyclic Carbonate Aminolysis. Polym Chem **2017**, 8 (41), 6349–6355. https://doi.org/10.1039/c7py01160a.

(46) Purwanto, N. S.; Chen, Y.; Torkelson, J. M. Reprocessable, Bio-Based, Self-Blowing Non-Isocyanate Polyurethane Network Foams from Cashew Nutshell Liquid. ACS Appl Polym Mater **2023**, 5 (8), 6651–6661. https://doi.org/10.1021/acsapm.3c01196.

(47) Sheppard, D. T.; Jin, K.; Hamachi, L. S.; Dean, W.; Fortman, D. J.; Ellison, C. J.; Dichtel, W. R. Reprocessing Postconsumer Polyurethane Foam Using Carbamate Exchange Catalysis and Twin-Screw Extrusion. ACS Cent Sci **2020**, 6 (6), 921–927. https://doi.org/10.1021/acscentsci.0c00083.

(48) Kim, S.; Li, K.; Alsbaiee, A.; Brutman, J. P.; Dichtel, W. R. Circular Reprocessing of Thermoset Polyurethane Foams. Advanced Materials **2023**, 35 (41), 2305387. https://doi.org/https://doi.org/10.1002/adma.202305387.